

University of Nebraska - Lincoln

DigitalCommons@University of Nebraska - Lincoln

Faculty Publications: Materials Research Science
and Engineering Center

Materials Research Science and Engineering Center

8-26-2004

First-principles study of adsorption of methanethiol on Co(0001)

Ligen Wang

University of Nebraska - Lincoln, lwang6@unl.edu

Evgeny Y. Tsybal

University of Nebraska-Lincoln, tsybal@unl.edu

Sitaram Jaswal

University of Nebraska, sjaswal1@unl.edu

Follow this and additional works at: <http://digitalcommons.unl.edu/mrsecfacpubs>



Part of the [Materials Science and Engineering Commons](#)

Wang, Ligen; Tsybal, Evgeny Y.; and Jaswal, Sitaram, "First-principles study of adsorption of methanethiol on Co(0001)" (2004).
Faculty Publications: Materials Research Science and Engineering Center. Paper 12.
<http://digitalcommons.unl.edu/mrsecfacpubs/12>

This Article is brought to you for free and open access by the Materials Research Science and Engineering Center at DigitalCommons@University of Nebraska - Lincoln. It has been accepted for inclusion in Faculty Publications: Materials Research Science and Engineering Center by an authorized administrator of DigitalCommons@University of Nebraska - Lincoln.

First-principles study of adsorption of methanethiol on Co(0001)

L. G. Wang, E. Y. Tsymbal, and S. S. Jaswal

Department of Physics and Astronomy and the Center for Materials Research and Analysis, University of Nebraska-Lincoln, Lincoln, Nebraska 68588-0111, USA

(Received 21 February 2004; revised manuscript received 10 May 2004; published 26 August 2004)

Investigation of the resident site and the adsorption phase structure of thiolates is of fundamental importance for understanding the formation of self-assembled organic monolayers on metal substrate surfaces. In the present study, we have investigated adsorption of methanethiol, CH_3SH , on the ferromagnetic Co(0001) surface using density functional theory calculations. We find that the dissociative adsorption of CH_3SH forming an adsorbed methylthiolate (CH_3S) and an adsorbed H atom is energetically favorable, and that the CH_3S molecule adsorbed at the threefold fcc and hcp hollow sites is most stable. The adsorption energy at the bridge site is only ~ 0.2 eV smaller than that at the threefold hollow site, and the adsorption of CH_3S at the atop site is unstable. For the $(\sqrt{3} \times \sqrt{3})\text{R}30^\circ$, (2×2) and (2×3) adsorptions, we find that the S-C bond tends to be normal to the surface, whereas for the (2×1) adsorption it tilts away from the surface normal direction by $\sim 40^\circ$. The (2×1) adsorption phase is much less stable. The reduction of the adsorption energy with the increasing coverage is attributed to the repulsive interaction between the adsorbates. Our calculations show that the $(\sqrt{3} \times \sqrt{3})\text{R}30^\circ$ structure may form in the process of methylthiolate adsorption on Co(0001) due to its adsorption energy being only 0.1 eV lower than that for the (2×2) and (2×3) structures. We find that there is a charge transfer from the substrate surface atoms to the S atoms, and that the S-Co bond is strongly polar. The surface Co atoms bound to S have a magnetic moment of $\sim 1.66\mu_B$, while the surface Co atoms unbound to S have a larger magnetic moment of $\sim 1.85\mu_B$. The S atom in the adsorbed CH_3S acquires a magnetic moment of $\sim 0.08\mu_B$.

DOI: 10.1103/PhysRevB.70.075410

PACS number(s): 68.43.-h, 71.15.Mb

I. INTRODUCTION

In recent years the formation of organic molecular self-assembled monolayers (SAMs) on metal substrate surfaces has attracted much attention.¹⁻³ Due to the possibility of controlling vertical and horizontal distributions of molecular chains with respect to the surface plane, the SAMs are attractive for various technological applications (see, e.g., Ref. 4, and references therein). They are also important for studying fundamental physical and chemical phenomena, such as surface reactions, the interface bonding between organic molecules and metal substrate atoms, and the influence of the interface atomic structure on electronic and transport properties. Recent experimental studies show the possibility of the controlled growth of organic molecular layers on magnetic metal substrates that opens new directions for using the SAMs, e.g., in spintronic applications.^{5,6} The functional properties of future devices based on organic/metal multilayers are largely controlled by the adsorption phase structure and the interface bonding. Therefore, understanding the adsorption mechanisms and the resulting electronic and atomic structure of the metal/adsorbate complexes is crucial for the functioning of these devices.

It has been well established that the organic molecule, such as methanethiol, deprotonates when adsorbed on various metal substrate surfaces at low temperatures.⁷⁻¹¹ However, there still exist many controversies on the adsorption site of thiolates, the adsorption phase structure, and whether or not the adsorbates dimerize. While the adsorption of CH_3S on the Ni(111),¹² Cu(111),^{11,13} and Au(111) (Refs. 9 and 14) surfaces was found both experimentally and theoretically to

occur at the threefold fcc or hcp hollow sites, other studies¹⁵⁻¹⁹ indicated that the bridge site on Au(111) is the most favorable site for adsorption. Furthermore, a chemical-shift normal incidence x-ray standing wave (CS-NIXSW) study found that methylthiolate can coadsorb on Cu(111) at the bridge site with the probability of 71% and at the fcc hollow site with the probability of 29%.¹⁰ This seems to be consistent with the cluster calculations²⁰ for methylthiolate adsorbed on unreconstructed Ni(111). These calculations predict that the three-coordinated fcc and hcp sites on Ni(111) have the nearly same adsorption energy as the bridge site, whereas the atop site is slightly less favorable. On the contrary, the thiolate species were found to adsorb at the atop site on Pt(111).²¹ The S-C bond axis is either normal to the surface^{9,17} or tilted away from the surface normal direction.^{10,12,16-18} A recent work by Ferral *et al.*¹³ emphasized that the bonding of the *n*-alkanethiols is independent of the chain length when the adsorbates are perpendicular to the surface. The authors also found a large charge transfer from the Cu(111) surface to the adsorbate.¹³ Several studies²²⁻²⁴ showed that the adsorbates form an adsorption structure of $(\sqrt{3} \times \sqrt{3})\text{R}30^\circ$. However, it was also argued²⁵ that the adsorption structure has a $c(4 \times 2)$ periodicity. *Ab initio* calculations by Vargas *et al.*¹⁶ found that the two adsorption structures on Au(111) are almost degenerate in energy, whereas Yourdshahyan and Rappe¹⁸ showed that an alternative $c(4 \times 2)$ model is energetically preferred over the $(\sqrt{3} \times \sqrt{3})\text{R}30^\circ$ adsorption structure. A metastable (3×4) ordered phase of methylthiolate on Au(111) was recognized recently by experiments and theory.²⁶ It is interesting that theoretical studies clearly indicated a dependence of the ad-

sorption energy on the coverage.^{16–18} Another longstanding issue is whether or not the adsorbed thiolates dimerize and adsorb as dimethyl disulfides on the substrate surfaces. Although some authors argued^{27,28} that there exists adsorption of disulfides, most experimental and theoretical studies^{9,16–18,26,29} suggest that the S-S bond tends to cleave resulting in thiolate adsorption on the substrate surfaces. *Ab initio* calculations showed that the cleavage of the S-S bond is energetically favorable.^{9,16,17}

In the present paper, we investigate the chemisorption of methanethiol on a ferromagnetic Co(0001) surface using density-functional calculations. This system is interesting because of the recent experimental attempts to grow the organic molecular SAMs, such as 1,1'-biphenyl-4,4'-dimethanethiol, on Co substrates aiming at spintronic applications.^{5,6} Due to a high dielectric constant and the possibility to control molecular chain distributions in the SAMs, this organic layer can be made very thin and, therefore, can serve as a dielectric barrier in magnetic tunnel junctions (for a recent review on magnetic tunnel junctions, see Ref. 30). Although methanethiol is a much simpler molecule compared to 1,1'-biphenyl-4,4'-dimethanethiol, the latter has the same headgroup, CH₃S, which bonds to a substrate. Similar to adsorption on other substrate surfaces, we find that the dissociative adsorption, forming an adsorbed CH₃S species and an H atom on Co(0001), is energetically preferred. Our calculations indicate that the threefold fcc and hcp hollow sites have nearly degenerate adsorption energy and are the most stable sites for adsorption of methylthiolate on Co(0001). The bridge site is higher in energy than the hollow sites by ~ 0.2 eV, and the adsorption of methylthiolate at the atop site is unstable. We find that the adsorption energy strongly depends on the coverage. From the adsorption energy results, we predict that the $(\sqrt{3} \times \sqrt{3})R30^\circ$ phase can be formed for methylthiolate adsorption on Co(0001). We infer that the repulsive interaction between the adsorbates is the reason for the adsorption energy reduction with increasing coverage. We find that there is a charge transfer from the substrate surface to the S atom in the adsorbed state, and that the S-Co bond is strongly polar. The surface Co(I) atoms bound to S have a magnetic moment of $\sim 1.66\mu_B$, while the surface Co(II) atoms not bound to S have a larger magnetic moment of $\sim 1.85\mu_B$. The S atom in the adsorbed CH₃S species acquires a magnetic moment of $\sim 0.08\mu_B$. Dimerization of the adsorbed CH₃S (i.e., forming adsorbed dimethyl disulfides) or the cleavage of the S-C bond in the adsorbed state (i.e., forming adsorbed S atom and gaseous CH₃) is found to be energetically unfavorable.

II. METHOD OF CALCULATIONS

We define the adsorption energy E_{ads} per molecule as follows:

$$E_{\text{ads}} = -\frac{1}{n} [E_{\text{tot}}(n - \text{molecule/substrate}) - E_{\text{tot}}(\text{substrate}) - nE_{\text{tot}}(\text{molecule})], \quad (1)$$

where n is the number of the adsorbed molecules, and

TABLE I. Theoretical and experimental values of surface relaxation, surface energy, and magnetic moments of the clean Co(0001) surface. Δd_{12} , Δd_{23} , and Δd_{34} denote the relative changes in the interlayer distances d_{12} , d_{23} , and d_{34} (see Fig. 1) compared to the bulk value of 2.03 Å. Previous FLAPW results and experimental values are given for comparison.

Property	This work	FLAPW ^a	Expt. ^b
relaxation			
$\Delta d_{12}(\%)$	-3.0		-2.1
$\Delta d_{23}(\%)$	+0.6		+1.3
$\Delta d_{34}(\%)$	-0.1		-0.2
surface energy			
$\gamma^{0001}(\text{J/m}^2)$	2.1	2.2	1.88 ^c
magnetic moment			
surface (μ_B)	1.76	1.76	
bulk (μ_B)	1.61	1.63	1.58 ^d

^aReference 38.

^bReference 37.

^cReference 39.

^dReference 40.

$E_{\text{tot}}(\text{substrate})$, $E_{\text{tot}}(\text{molecule})$, and $E_{\text{tot}}(n - \text{molecule/substrate})$ are the total energies of the clean substrate, the gas-phase molecule, and the interacting surface and adsorbed-molecule system, respectively. These total energies are obtained by performing spin-polarized calculations using the pseudopotential plane-wave method^{31,32} in the framework of density-functional theory with the generalized gradient approximation (GGA) for the exchange-correlation potential.³³ We use a slab model to simulate the surface adsorption: the slab includes 5 Co atomic layers and a vacuum region equivalent to 12 atomic layers. The Co(0001) substrate is unreconstructed. We put the adsorbed molecule on one side of the slab. The atoms in the substrate (except for the two bottom layers) and in the adsorbed organic molecule are allowed to relax. The Vanderbilt ultrasoft pseudopotentials,³⁴ which include 9, 6, 4, and 1 valence electrons for Co, S, C, and H, respectively, are employed to represent the interaction of the core and valence electrons in these atoms. The electronic wave functions are expanded in a plane-wave basis set with the energy cutoff of 350 eV. We use special \mathbf{k} points³⁵ for the surface Brillouin zone integration equivalent to fourteen special \mathbf{k} points in the irreducible part of the Brillouin zone of a (1×1) surface unit cell. Our theoretical lattice constants ($a=2.50$ Å and $c=4.06$ Å) for hcp Co compare well with the experimental values ($a=2.51$ Å and $c=4.07$ Å).³⁶ As a further check of the parameters used, we calculate the surface relaxation, surface energy and magnetic properties of the clean Co(0001), and the results are presented in Table I. As one can see from the table, our theoretical surface relaxation values are in good agreement with the experimental values.³⁷ Both theory and experiment predict oscillating interlayer-distance relaxation with a first layer-spacing contraction. The surface energy and the magnetic moments are consistent with the results obtained from the FLAPW calculations³⁸ and are in reasonable

agreement with the experimental values.^{39,40} We also check the adsorption energies by putting the molecules on both sides of a 9-atomic layer slab with the central layer fixed as the bulk lattice. Our tests show that the adsorption energies are convergent to an accuracy of 0.2 eV/molecule with respect to \mathbf{k} points, energy cutoff, and slab thickness. Since we are interested in the relative stability of various adsorption sites, we always compare the energies in the same adsorption structure with the adsorbed molecule at different sites. Therefore, the energy difference between two occupation sites should converge to a better accuracy than 0.2 eV.

III. RESULTS AND DISCUSSION

First, we consider intact adsorption of methanethiol on Co(0001). We find that CH_3SH always relaxes away from the surface, i.e., the adsorbed $\text{CH}_3\text{SH}/\text{Co}(0001)$ state is energetically unfavorable. Therefore, methanethiol does not molecularly adsorb on the Co(0001) surface. Next, we consider dissociative adsorption of methanethiol, and find that breaking the S-H bond to form an adsorbed methylthiolate CH_3S molecule and an adsorbed H atom on the substrate surface is energetically favorable. The dissociative adsorption state is 1.4 eV lower in energy than the infinitely separated state [i.e., the clean Co(0001) plus a free or gas-phase methanethiol]. This is consistent with the theoretical calculations for methanethiol adsorption on other substrate surfaces.⁹ Experiments also show that methanethiol deprotonates when it adsorbs on the substrate surface at low temperatures.^{7,8,10,11} Furthermore, we find that dimerization of adsorbates on the surface (i.e., forming adsorbed dimethyl disulfides $\text{CH}_3\text{S}-\text{SCH}_3$) is energetically unfavorable. Therefore, in the present study we focus on investigating the adsorption site and adsorption structure of methylthiolate on Co(0001).

We consider four adsorption sites, i.e., the fcc, hcp, bridge, and atop sites, which may be occupied by the thiolate CH_3S on the Co(0001) surface. The adsorption phase structure is assumed to be (1×1) , (2×1) , $(\sqrt{3} \times \sqrt{3})\text{R}30^\circ$, (2×2) or (2×3) , corresponding to the coverage θ varying between 1 and $\frac{1}{6}\text{ML}$ ($\theta=1\text{ML}$ means one CH_3S molecule per one surface Co atom). The adsorption sites and surface unit cells of the adsorption structures are shown in Fig. 1.

We find that the (1×1) structure is unstable, i.e., it has a negative adsorption energy, no matter on which site we put the thiolate species. For other adsorptions, we find that the adsorption energy is always positive when the methylthiolate adsorbs at the threefold fcc and hcp hollow sites. The threefold fcc and hcp hollow sites are found to be the most stable adsorption sites and have nearly same adsorption energies. This is easy to understand because the two adsorption structures are different from each other only starting from the third layer. The bridge site is unstable for the (2×1) adsorption. The bridge site is not a local minimum for the (2×2) adsorption because, if we do not constrain the relaxation, the CH_3S molecule always goes to the threefold fcc or hcp hollow site. However, the unconstrained relaxation only results in the adsorbed species to move to a threefold hollow site.

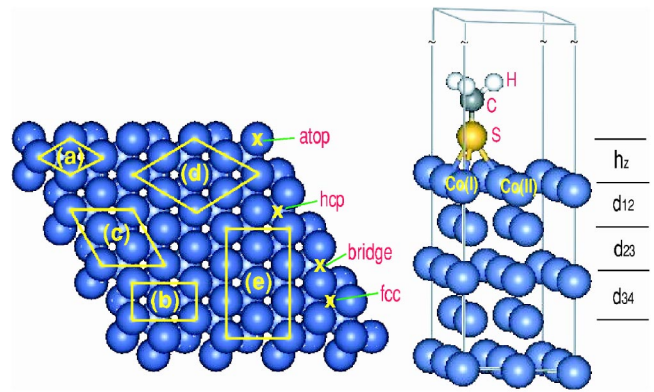


FIG. 1. (Color online) Surface unit cells and adsorption sites (left panel): (a) (1×1) , (b) (2×1) , (c) $(\sqrt{3} \times \sqrt{3})\text{R}30^\circ$, (d) (2×2) , and (e) (2×3) . The right panel shows an example of the (2×2) adsorption supercell with methylthiolate adsorbed at the hcp hollow site. The Co, S, C, and H atoms are represented by the largest, second largest, third largest, and smallest spheres, respectively. Co(I) denotes the surface Co atoms bound to S, whereas Co(II) denotes the surface Co atoms unbound to S in the surface unit cell.

This is different from the previous prediction that the most stable site for CH_3S adsorption on Au(111) is located between the bridge site and the hollow site.^{16–18} We do not find such a low energy site between the bridge and three-coordinated hollow sites for the CH_3S adsorption on Co(0001). In contrast, for the $(\sqrt{3} \times \sqrt{3})\text{R}30^\circ$ adsorption the bridge site is a local minimum with an adsorption energy higher by ~ 0.2 eV than that at the threefold fcc or hcp hollow site.

The optimized atomic geometry and the adsorption energy are presented in Table II. We consider two high symmetry orientations for the hydrogen atoms in adsorbed methylthiolate, i.e., the so-called staggered and eclipsed orientations [see Fig. 4(a) of Ref. 18], and find that the energy difference between the two orientations is ~ 1 meV, being less than the accuracy of our calculation. For the $(\sqrt{3} \times \sqrt{3})\text{R}30^\circ$, (2×2) and (2×3) adsorptions, we find that the S-C bond prefers to be normal to the surface. For the (2×2) adsorption at the fcc hollow site, we calculated the dependence of the adsorption energy on the S-C bond tilt angle. Our results indicate that it has the lowest energy (or the largest adsorption energy) when the S-C bond is normal to the surface. The S-Co bond lengths are longer when the CH_3S molecule adsorbs at the threefold hollow sites compared to those at the bridge site. The S-C bond tilts away from the surface normal direction only for the (2×1) adsorption (see Table II). The three S-Co bonds in this adsorption structure have very different bond lengths, and the S atom position h_z is higher than for other adsorptions.

The adsorption energy is found to depend on the coverage. Figure 2 shows the adsorption energy for various adsorption structures with CH_3S at the fcc hollow site. We find that the adsorption energy approaches a constant value when the coverage is smaller than $\frac{1}{4}\text{ML}$. The adsorption energy for the $(\sqrt{3} \times \sqrt{3})\text{R}30^\circ$ structure is slightly lower than that for the (2×2) and (2×3) structures. However, the (2×1) adsorption is much less stable. Previous studies suggested that sur-

TABLE II. Optimized atomic geometry and adsorption energy for various adsorption structures. $\theta = 1$ ML corresponds to one methylthiolate molecule per a surface Co atom. “Unrelaxed” means that the relaxation of the Co atoms on the substrate surface is not allowed, whereas “constrained” means the S atom is fixed at the bridge site, whereas all other atoms in the substrate and adsorbate are allowed to relax. h_z stands for the vertical distance between the S atom and the relaxed clean surface plane. ϕ is the tilt angle of the S-C bond away from the surface normal direction.

	θ (ML)	h_z (Å)	d_{S-Co} (Å)	d_{S-C} (Å)	ϕ (°)	E_{ads} (eV)
(2×1)						
fcc	$\frac{1}{2}$	1.83	2.18 2.21 2.45	1.91	42.8	0.57
fcc (unrelaxed)	$\frac{1}{2}$					0.25
hcp	$\frac{1}{2}$	1.82	2.18 2.20 2.37	1.87	36.6	0.45
bridge	$\frac{1}{2}$					unstable
($\sqrt{3} \times \sqrt{3}$)R30°						
fcc	$\frac{1}{3}$	1.67	2.22 2.22 2.22	1.85	0	2.92
hcp	$\frac{1}{3}$	1.68	2.21 2.21 2.21	1.84	0	2.92
bridge	$\frac{1}{3}$	1.66	2.17 2.17	1.85	0	2.73
(2×2)						
fcc	$\frac{1}{4}$	1.67	2.20 2.20 2.20	1.85	0	3.05
fcc (unrelaxed)	$\frac{1}{4}$					3.00
hcp	$\frac{1}{4}$	1.67	2.20 2.20 2.20	1.85	0	3.03
bridge (constrained)	$\frac{1}{4}$	1.56	2.16 2.16	1.86	0	2.81
(2×3)						
fcc	$\frac{1}{6}$	1.68	2.20 2.20 2.20	1.84	0	3.05

face atom relaxation is responsible for the dependence of the adsorption energy on the coverage.¹⁶ To check this prediction we calculated the adsorption energy for the 0.5 ML [corresponding to the (2×1) structure] and 0.25 ML [corresponding to the (2×2) structure] coverages without allowing the surface atoms to relax. The results given in Table II and Fig. 2 (star symbols) show that the surface atom relaxation has very small effect on the dependence of the adsorption energy on the coverage. We infer from this that the adsorption energy reduction with increasing coverage is due to the repulsive interaction between the adsorbed methylthiolates. Similarly, the repulsive interaction between the adsorbed oxygen

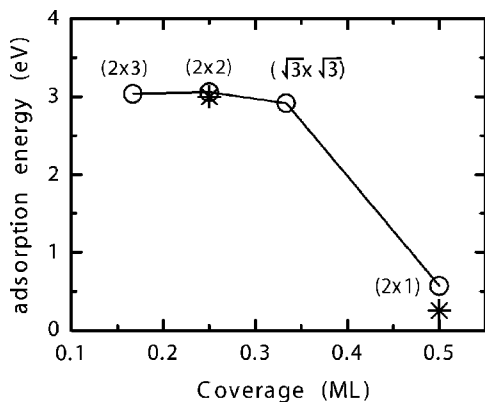


FIG. 2. Adsorption energy for various adsorption phase structures with methylthiolate adsorbed at the fcc hollow site. For the ‘unrelaxed’ case (see explanation in the caption to Table II) the adsorption energy is represented by the star symbol.

atoms was used to explain the dependence of adsorption energy on the coverage for oxygen adsorption on Ru(0001) (Ref. 41) and Ag(111).⁴² The fact that the ($\sqrt{3} \times \sqrt{3}$)R30° ordered phase has the adsorption energy close to that for the (2×2) and (2×3) structures suggests that there is no significant repulsive interaction between the adsorbates in this phase. Unlike the previous calculations performed for the adsorption of CH₃S on Au(111),^{16–18} we do not find that the bridge site is the most stable site for adsorption of CH₃S on Co(0001). Therefore, we predict that the $c(4 \times 2)$ (3×4) phases will not form for CH₃S adsorption on Co(0001).

The magnetic moments and the spin projected charge populations are presented in Table III. First, we see that the surface Co atom has a magnetic moment of $1.76\mu_B$, which is larger than the magnetic moment for the bulk, $1.61\mu_B$, due to the narrowing of the 3d electron bands at the surface. This magnetic moment value is in excellent agreement with the previous FLAPW calculations³⁸ (see Table I). There exists two types of surface Co atoms for the CH₃S-adsorbed surface, which have distinct magnetic moments. Co(I) atoms bound to the S atom of CH₃S have a magnetic moment of $\sim 1.66\mu_B$, which is smaller than that on the clean-surface atoms, whereas Co(II) atoms, which are next to Co(I) and unbound to S, have a larger magnetic moment of $\sim 1.85\mu_B$. The difference in magnetic moments mostly results from the difference in the minority spin population since its change is twice as much as the population change for the majority spin. We note that Co(I) have the total number of valence electrons close to that they have in the bulk, and Co(II) have the total number of valence electrons close to that they have on

TABLE III. Spin projected charge populations and magnetic moments within each atomic sphere of the Co and S atoms for bulk hcp Co, clean Co(0001), and adsorbed Co(0001).

		<i>s</i>	<i>p</i>	<i>d</i>	tot	tot($\uparrow+\downarrow$)	<i>M</i> (μ_B)
bulk hcp Co							
Co	\uparrow	0.22	0.20	4.45	4.87	8.13	1.61
	\downarrow	0.23	0.25	2.78	3.26		
clean surface							
Co	\uparrow	0.21	0.16	4.52	4.89	8.02	1.76
	\downarrow	0.23	0.22	2.68	3.13		
$(\sqrt{3}\times\sqrt{3})R30^\circ$							
Co(I)	\uparrow	0.21	0.20	4.49	4.90	8.13	1.67
	\downarrow	0.22	0.23	2.78	3.23		
S	\uparrow	0.69	1.38	0.08	2.15	4.22	0.08
	\downarrow	0.68	1.30	0.09	2.07		
(2×2)							
Co(I)	\uparrow	0.21	0.21	4.48	4.90	8.14	1.66
	\downarrow	0.22	0.24	2.78	3.24		
Co(II)	\uparrow	0.21	0.17	4.56	4.94	8.02	1.86
	\downarrow	0.22	0.21	2.65	3.08		
S	\uparrow	0.70	1.36	0.09	2.15	4.23	0.07
	\downarrow	0.68	1.31	0.09	2.08		
(2×3)							
Co(I)	\uparrow	0.21	0.21	4.47	4.89	8.12	1.66
	\downarrow	0.22	0.24	2.77	3.23		
Co(II)	\uparrow	0.22	0.17	4.55	4.94	8.03	1.85
	\downarrow	0.23	0.21	2.65	3.09		
S	\uparrow	0.70	1.36	0.09	2.15	4.22	0.08
	\downarrow	0.68	1.31	0.09	2.07		

the clean surface. The exchange splitting of the Co 3*d* bands induces a magnetic moment of about $0.08\mu_B$ at the S atom. We see, therefore, that the bonding between the surface Co atoms and the S atoms does not quench the interface magnetism. This is similar to the prediction obtained for the

Co/Al₂O₃ interface⁴³ and offers the possibility to use magnetic junctions with the Co/organic interfaces in spintronic applications.

Figure 3 shows the total valence electron density and the difference electron density for the $(\sqrt{3}\times\sqrt{3})R30^\circ$ adsorption with the hydrogen atoms having the eclipsed orientation.¹⁸ We see that the electron density around the surface Co atoms is depleted, while there is a significant enhancement of the electron density at the Co-S bond close to the S atom. This is similar to the adsorption of CH₃S on Au(111) (Refs. 9 and 15) and Cu(111) (Ref. 13) substrates, in which the metal-S bond is found to be strongly polar with a charge accumulation near the S atom and a depletion near the metal atom along the bond. By comparing the number of electrons in the atomic sphere around the S atom in the adsorbed and gas-phase CH₃S, we find that there is a charge transfer from the surface Co atoms to the S atom. The S atom gains 0.22 electrons from the substrate surface for the $(\sqrt{3}\times\sqrt{3})R30^\circ$ and (2×2) adsorptions, which is similar to a net excess charge of ~ 0.3 electrons for the CH₃S adsorption on Au(111) compared to the free radical.⁹ Similar to the O 2*p* antibonding state for oxygen adsorption on Ag(111),⁴² we find that the S 3*p* antibonding state is largely occupied, which reduces the strength of the covalent bonding between Co and S. However, there is a much stronger hybridization interaction between the Co 3*d* and S 3*p* orbitals than the interaction between the Au 5*d* and S 3*p* orbitals because the Co 3*d* states lie higher in energy than the Au 5*d* states. Therefore, the Co-S bond is stronger than the Au-S bond, which explains why adsorption of CH₃S on Co(0001) has a much larger adsorption energy of 3.0 eV compared to ~ 2 eV for adsorption on Au(111).⁹ Figure 3 also demonstrates that the perturbation due to adsorption is mainly in the topmost Co layer, which is consistent with the small difference in the adsorption energy between the two threefold hollow sites.

Our calculations also indicate that breaking the S-C bond in the adsorbed CH₃S to form the adsorbed S atom and free CH₃ is energetically unfavorable. Therefore, at low temperatures it is impossible to cleave the S-C bond and form adsorbed S atoms and gas-phase CH₃. This is consistent with

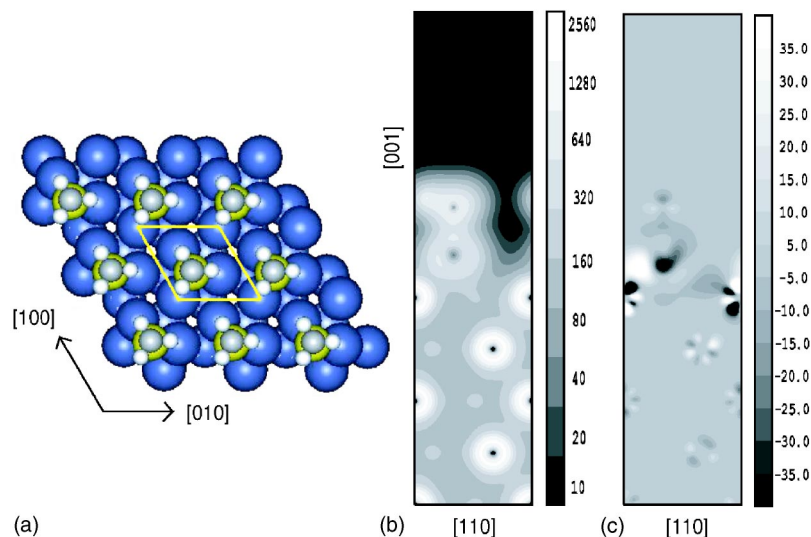


FIG. 3. (Color online) (a) Optimized atomic structure (topview), (b) total valence electron density, and (c) difference electron density for the $(\sqrt{3}\times\sqrt{3})R30^\circ$ adsorption with CH₃S at the fcc hollow site. The difference electron density is defined by $\Delta\rho = \rho(\text{CH}_3\text{S}/\text{substrate}) - \rho(\text{substrate}) - \rho(\text{CH}_3\text{S})$.

the experiments in which adsorbed S atoms were observed only at high temperatures.^{11,27}

IV. SUMMARY

We have performed spin-polarized total energy calculations for adsorption of methanethiol on the magnetic Co(0001) substrate. The most interesting issues such as the adsorption site and the adsorption phase structure have been carefully investigated. For the clean Co(0001) surface, our results for the surface relaxation, surface energy and magnetic moments are in excellent agreement with available experimental values and previous FLAPW calculations. We find that in the process of adsorption methanethiol tends to deprotonate, i.e., breaks the S-H bond to form methylthiolate CH_3S , which adsorbs on Co(0001). The most stable adsorption sites for adsorption of CH_3S on Co(0001) are the threefold fcc and hcp hollow sites. The adsorption energy at the bridge site is ~ 0.2 eV smaller than that at the threefold hollow site, and it is unstable when CH_3S adsorbs at the atop site. For the $(\sqrt{3} \times \sqrt{3})\text{R}30^\circ$, (2×2) and (2×3) adsorption structures, we find that the S-C bond tends to be normal to the surface, whereas for the (2×1) adsorption structure it tilts away from the surface normal direction by $\sim 40^\circ$. The

adsorption energy decreases when the coverage of CH_3S increases. This is attributed to the repulsive interaction between the adsorbates. We predict that the $(\sqrt{3} \times \sqrt{3})\text{R}30^\circ$ adsorption structure may be formed for methylthiolate adsorption on Co(0001) since the adsorption energy is only 0.1 eV lower than that for the (2×2) and (2×3) structures. Our calculations indicate that there is a charge transfer from the substrate surface atoms to the S atom, and that the S-Co bond is strongly polar. There exist two types of the surface Co atoms upon adsorption: Co(I), which are bound to S of CH_3S , have a magnetic moment of $\sim 1.66\mu_B$ and Co(II), which are next to Co(I) and unbound to S, have a larger magnetic moment of $\sim 1.85\mu_B$. This magnetic moment difference mostly results from the difference in the minority spin populations. The induced magnetic moment on the S atom in the adsorbed CH_3S is $\sim 0.08\mu_B$.

ACKNOWLEDGMENTS

We are grateful to our colleagues Peter Dowben and Tony Caruso for useful discussions. This work is supported by NSF-MRSEC (Grant No. DMR-0213808), NSF (Grant No. DMR-0203359), and the Nebraska Research Initiative. The calculations were performed utilizing the Research Computing Facility of the University of Nebraska-Lincoln.

-
- ¹L. H. Dubois and R. G. Nuzzo, *Annu. Rev. Phys. Chem.* **43**, 437 (1992).
²A. Ulman, *Chem. Rev. (Washington, D.C.)* **96**, 1533 (1996).
³G. E. Poirier, *Chem. Rev. (Washington, D.C.)* **97**, 1117 (1997).
⁴S. V. Atre, B. Lieberg, and D. L. Allara, *Langmuir* **11**, 3882 (1995).
⁵A. N. Caruso, R. Rajesekaran, J. Redepenning, Y. B. Losovyj, and P. A. Dowben, *Mater. Res. Soc. Symp. Proc.* **775** (in press).
⁶A. N. Caruso, R. Rajesh, G. Gallup, J. Redepenning, and P. A. Dowben, *J. Phys.: Condens. Matter* **16**, 1 (2004).
⁷S. Bao, C. F. McConville, and D. P. Woodruff, *Surf. Sci.* **187**, 133 (1987).
⁸M. E. Castro and J. M. White, *Surf. Sci.* **257**, 22 (1991).
⁹H. Gröbeck, A. Curioni, and W. Andreoni, *J. Am. Chem. Soc.* **122**, 3839 (2000).
¹⁰R. L. Toomes, M. Polcik, M. Kittel, J.-T. Hoefft, D. I. Sayago, M. Pascal, C. L. A. Lamont, J. Robinson, and D. P. Woodruff, *Surf. Sci.* **513**, 437 (2002).
¹¹G. J. Jackson, D. P. Woodruff, R. G. Jones, N. K. Singh, A. S. Y. Chan, B. C. C. Cowie, and V. Formoso, *Phys. Rev. Lett.* **84**, 119 (2000).
¹²D. R. Mullins, D. R. Huntley, T. Tang, D. K. Saldin, and W. T. Tysoe, *Surf. Sci.* **380**, 468 (1997).
¹³A. Ferral, P. Paredes-Olivera, V. A. Macagno, and E. M. Patrito, *Surf. Sci.* **525**, 85 (2003).
¹⁴Y. Yourdshahyan, H. K. Zhang, and A. M. Rappe, *Phys. Rev. B* **63**, 081405(R) (2001).
¹⁵H. Häkkinen, R. N. Barnett, and U. Landman, *Phys. Rev. Lett.* **82**, 3264 (1999).
¹⁶M. C. Vargan, P. Giannozzi, A. Selloni, and G. Scoles, *J. Phys. Chem. B* **105**, 9509 (2001).
¹⁷T. Hayashi, Y. Morikawa, and H. Nozoye, *J. Chem. Phys.* **114**, 7615 (2001).
¹⁸Y. Yourdshahyan and A. M. Rappe, *J. Chem. Phys.* **117**, 825 (2002).
¹⁹L. G. Wang, E. Y. Tsymlal, and S. S. Jaswal (unpublished).
²⁰H. Yang, T. C. Caves, J. L. Whitten, and D. R. Huntley, *J. Am. Chem. Soc.* **116**, 8200 (1994).
²¹J. J. Lee, C. J. Fisher, C. Bittencourt, D. P. Woodruff, A. S. Y. Chan, and R. G. Jones, *Surf. Sci.* **516**, 1 (2002).
²²M. G. Samant, C. A. Brown, and J. G. Gordon, *Langmuir* **7**, 437 (1991).
²³S. S. Kim, Y. Kim, H. I. Kim, S. H. Lee, T. R. Lee, S. S. Perry, and J. W. Rabalais, *J. Chem. Phys.* **109**, 9574 (1998).
²⁴C. E. D. Chidsey and D. N. Loiacono, *Langmuir* **6**, 682 (1990).
²⁵N. Camillone, C. E. D. Chidsey, G. Liu, and G. Scoles, *J. Chem. Phys.* **98**, 3503 (1993).
²⁶V. De Renzi, R. Di Felice, D. Marchetto, R. Biagi, U. del Pennino, and A. Selloni, *J. Phys. Chem. B* **108**, 16 (2004).
²⁷G. Liu, J. A. Rodriguez, J. Dvorak, J. Hrbek, and T. Jirsak, *Surf. Sci.* **505**, 295 (2002).
²⁸G. J. Kluth, C. Carraro, and R. Maboudian, *Phys. Rev. B* **59**, R10 449 (1999).
²⁹R. G. Nuzzo, B. R. Zegarski, and L. H. Dubois, *J. Am. Chem. Soc.* **109**, 733 (1987).
³⁰E. Y. Tsymlal, O. N. Mryasov, and P. R. LeClair, *J. Phys.: Condens. Matter* **15**, R109 (2003).
³¹M. C. Payne, M. P. Teter, D. C. Allan, T. A. Arias, and J. D. Joannopoulos, *Rev. Mod. Phys.* **64**, 1045 (1992).
³²G. Kresse and J. Hafner, *Phys. Rev. B* **47**, 558 (1993); **49**, 14 251

- (1994); G. Kresse and J. Furthmüller, *Comput. Mater. Sci.* **6**, 15 (1996); *Phys. Rev. B* **54**, 11 169 (1996).
- ³³J. P. Perdew, in *Electronic Structure of Solids '91*, edited by P. Ziesche and H. Eschring (Akademie-Verlag, Berlin, 1991); J. P. Perdew, J. A. Chevary, S. H. Vosko, K. A. Jackson, M. R. Pederson, D. J. Singh, and C. Fiolhais, *Phys. Rev. B* **46**, 6671 (1992).
- ³⁴D. Vanderbilt, *Phys. Rev. B* **41**, 7892 (1990).
- ³⁵H. J. Monkhorst and J. D. Pack, *Phys. Rev. B* **13**, 5188 (1976).
- ³⁶C. Kittel, *Introduction to Solid State Physics* (Wiley, New York, 1971).
- ³⁷J. Lahtinen, J. Vaari, T. Vaara, K. Kauraala, P. Kaukasoina, and M. Lindroos, *Surf. Sci.* **425**, 90 (1999).
- ³⁸C. Li, A. J. Freeman, and C. L. Fu, *J. Magn. Magn. Mater.* **94**, 134 (1991).
- ³⁹L. E. Murr, *Interfacial Phenomena in Metals and Alloys* (Addison-Wesley, Reading, 1975), Table 3.4, pp. 101–106. The experimental values are surface energies at the melting point; therefore, one can expect that the 0 K values are about 10% higher [S. P. Chen, *Surf. Sci. Lett.* **264**, L162 (1992)].
- ⁴⁰H. P. Meyers and W. Sucksmith, *Proc. R. Soc. London, Ser. A* **207**, 427 (1951).
- ⁴¹C. Stampfl, S. Schwegmann, H. Over, M. Scheffler, and G. Ertl, *Phys. Rev. Lett.* **77**, 3371 (1996); C. Stampfl and M. Scheffler, *Phys. Rev. B* **54**, 2868 (1996).
- ⁴²W. X. Li, C. Stampfl, and M. Scheffler, *Phys. Rev. B* **65**, 075407 (2002).
- ⁴³I. I. Oleinik, E. Y. Tsybal, and D. G. Pettifor, *Phys. Rev. B* **62**, 3952 (2000).